



ELSEVIER

Applied Surface Science 174 (2001) 275–282

www.elsevier.nl/locate/apsusc

Ion-induced nitridation of GaAs(1 0 0) surface

Y.G. Li, A.T.S. Wee*, C.H.A. Huan, J.C. Zheng

Department of Physics, National University of Singapore, Lower Kent Ridge Road, Singapore 119260, Singapore

Received 28 September 2000; accepted 10 February 2001

Abstract

The ion-induced nitridation of GaAs(1 0 0) using 1.2 keV N_2^+ ion beams has been investigated using in situ X-ray photoelectron spectroscopy (XPS) and atomic force microscopy (AFM). Ga-rich surfaces produced by Ar^+ cleaning, promote initial nitridation and formation of GaN. The dependence of $[N]/[Ga]$ and $[As]/[Ga]$ atomic ratios on substrate temperature, nitridation time, and nitrided layer depth suggest that the process is self-limiting. The degree of nitridation increases with the temperature, but decreases again at higher temperatures ($>450^\circ C$). Smooth nitrided layers are formed between room temperature and $450^\circ C$. For nitridation at $T = 600^\circ C$ however, the aggregation of $GaAs_{1-x}N_x$ results in the roughening of the nitrided surfaces. Diffusion, sputtering, and decomposition effects in the nitridation process are considered, and the mechanisms of $GaAs_{1-x}N_x$ formation are discussed. © 2001 Elsevier Science B.V. All rights reserved.

PACS: 61.80.Jh; 61.82.Fk; 81.05.Ea

Keywords: Ion beam; Nitridation; Gallium nitride; GaAs(1 0 0); XPS; AFM

1. Introduction

Group III–V nitrides, which have room temperature band gaps ranging from 1.9 eV for InN to 3.4 eV for GaN, and to 6.2 eV for AlN, are attractive for optoelectronic devices emitting in the blue and UV wavelengths. They are also the most promising material system for high-temperature and high-power devices due to their excellent thermal properties. Moreover, with its large saturated electron drift velocity, GaN is a suitable candidate for high-frequency devices [1]. To date, many techniques, including metalorganic chemical vapor deposition (MOCVD), reactive sputtering, molecular-beam epitaxy (MBE), metal-organic vapor-phase epitaxy (MOVPE), plasma deposition,

and chemical beam epitaxy (CBE) have been used to grow GaN thin films on sapphire, SiC, and GaAs substrates [2–5]. However, the optimization of the initial growth of GaN is critical, because of the large lattice mismatch between the substrates (such as Si, SiC, sapphire, and GaAs) and GaN layer. Furthermore, surface stoichiometry is a major parameter controlling the phase purity and hence GaN growth kinetics and morphology [6]. The use of a buffer layer prior to epitaxial growth, especially on sapphire, SiC [7], GaAs [8,9], and Si [10,11] has therefore recently received much attention. Nucleation of GaN by N-ion implantation in GaAs [12] is an alternative method for the nucleation of GaN at lower temperatures. Although the ability to grow thin films on elemental semiconductors such as Si [13] and Ge [14] surfaces by N^+ or N_2^+ ion beam bombardment is well documented, the nucleation of binary compound GaN is

* Corresponding author. Tel.: +65-8746362; fax: +65-7776126.
E-mail address: phyweets@nus.edu.sg (A.T.S. Wee).

more complex. Furthermore, surface damage should be minimized during N-ion implantation in order to decrease the mismatch between initial nitride layer and subsequent GaN film. GaN is thermodynamically more stable than GaAs (heats of formation ≈ -109.5 and -81.5 kJ mol $^{-1}$, respectively [15]). Implantation of N $_2^+$ in GaAs is expected to cause N–As exchange forming GaN on the surface of GaAs. Since As is more volatile than Ga, it tends to evaporate from GaAs upon thermal annealing and ion bombardment, thereby facilitating the replacement of As by N atoms. Previous works on ion beam nitridation of GaAs have indeed reported that Ga was preferentially nitrided as compared with As [15–17].

In the present study, in situ XPS is used to monitor the chemical state and compositional changes to a GaAs(1 0 0) surface as a function of N ion dose at temperatures up to 600°C. The N 1s, Ga 3d, and As 3d core level intensities and binding energies of the nitrogen ion bombarded Ar $^+$ -cleaned GaAs(1 0 0) surfaces are compared. Our results suggest the formation of thermally stable thin GaN films on the GaAs(1 0 0) surfaces. XPS depth profiling of the nitride layers is used to analyze the chemical composition as a function of depth. AFM is used to investigate the morphology of the ion-bombarded surfaces and measure the surface roughness.

2. Experimental

The experiments were carried out in a home-built twin-chamber ultrahigh vacuum (UHV) system equipped with a growth chamber and an analysis chamber equipped with XPS (VG XR3E2 dual anode X-ray sources, EA125 hemispherical energy analyzer). The silicon-doped n-type GaAs(1 0 0) samples with carrier concentrations between 1×10^{18} and 2.6×10^{18} cm $^{-3}$ were cleaned ultrasonically with methanol. Subsequently, they were cleaned by hydrofluoric acid in ethanol, followed by de-ionized water. They were then rinsed with acetone and dried in flowing Ar. The chemically cleaned samples were mounted onto a tantalum plate and introduced into the growth chamber via a fast entry lock. An AG21 cold cathode ion gun in the growth chamber was used to produce 1 keV, 18 μ A Ar $^+$ ion beam for removal of oxygen and carbon contamination prior to GaAs

nitridation under 1.2 keV N $_2^+$ 16 μ A at 5.5×10^{-6} mbar. The samples were maintained at various temperatures between room temperature and 600°C during ion-induced nitridation. After nitridation, the samples were transferred to the XPS chamber. In situ XPS measurements of samples were performed when the samples were cooled to room temperature.

In situ XPS analysis was performed using a Mg K α source (1253.6 eV) at incident angle of 55° (normal detection) to acquire spectra of the N 1s, Ga 3d, and As 3d photoelectron spectra. The XPS depth profile analysis (Mg K α 1253.6 eV at incident angle of 45° and normal detection) was carried out in a VG ESCA-LAB220i-XL. An Ar $^+$ beam is employed during sputtering of the nitrided GaAs(1 0 0) surfaces, and the spectra of N 1s, Ga 3d, and As 3d are recorded at different sputtering times until bulk GaAs is reached. Mixed Gaussian–Lorentzian (at 80% Gaussian) curves were used to fit the spectra.

To minimize the effects of oxidation of the nitrided layer surfaces during ex situ AFM analysis, AFM images of the nitrided GaAs surfaces were recorded immediately after the samples were taken out from the UHV system. All AFM images were recorded in the tapping mode on a Digital Instruments D3000 AFM system.

3. Results and discussion

3.1. Formation of the nitrided films

Fig. 1(a) shows the Ga 3d and As 3d XPS narrow scans of ultrasonically cleaned GaAs(1 0 0) surface, showing the surface oxide peaks Ga $_2$ O $_3$ with Ga 3d binding energy of 20.1 ± 0.1 eV and As $_2$ O $_3$ at the As 3d binding energy of 44.2 ± 0.1 eV. To remove the contamination completely, 5 min of 1 keV, 18 μ A Ar $^+$ ion sputtering at room temperature was found to be sufficient, as shown in Fig. 1(b). The As 3d spectra can be fitted with two peaks that are assigned to As 3d $_{5/2}$ (40.8 ± 0.2 eV, FWHM = 1.2 ± 0.1 eV) and As 3d $_{3/2}$ (41.5 ± 0.2 eV, FWHM = 1.2 ± 0.1 eV), with a spin-orbit splitting of 0.69 eV and a branching ratio 3d $_{3/2}$:3d $_{5/2}$ of 0.60 [18]. The results of the Ga 3d and As 3d curve-fitted XPS analysis in Fig. 1(b) imply that a Ga-rich surface with [As]/[Ga] atomic ratio of 0.96 was obtained, after the GaAs surface was cleaned

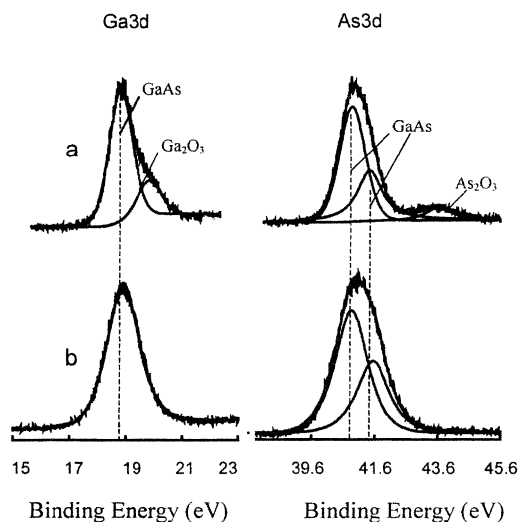


Fig. 1. XPS spectra of the Ga 3d and As 3d peaks for: (a) solution cleaned GaAs; (b) 1 keV, 18 μ A Ar^+ -bombarded GaAs in 5 min.

by Ar ion beam sputtering. Similar results were reported by other authors [12,16,19].

Before N_2^+ bombardment, GaAs surfaces are cleaned by 1 keV, 18 μ A Ar^+ ion sputtering at room temperature for 5 min, resulting in a clean surface as shown in Fig. 2(a). Fig. 2(b)–(e) show XPS spectra of the Ga 3d, As 3d, and N 1s peaks after 1.2 keV N_2^+ bombardment at 300°C for 5, 15, 25, and 60 min, respectively. The Ga 3d spectra after N_2^+ bombardment broadened and shifted to higher binding energies (BE). This is due to the contribution from Ga–N bonds formed on GaAs. The Ga 3d contributions are attributed to Ga–N (19.5 ± 0.1 eV, FWHM = 1.2 ± 0.1 eV) and GaAs (18.8 ± 0.1 eV, FWHM = 1.2 ± 0.1 eV) [18,19]. The binding energies for As 3d_{5/2} and As 3d_{3/2} show no change in their peak positions compared to that of the clean surface (see Fig. 2(a)). We could not observe any other bonding states in the As 3d level that could suggest that an As–N bond may have formed. The N 1s spectra can be fitted by one peak at a binding energy of 397.0 ± 0.2 eV and FWHM of 1.5 ± 0.1 eV, which is consistent with the formation of Ga–N bonds on GaAs [18]. It can be seen in Fig. 2 that the concentration of Ga–N bonds in the nitrided layers increases with nitridation time.

Fig. 3(a)–(e) show the Ga 3d, As 3d, and N 1s spectra of clean GaAs, as well as after 1.2 keV N_2^+ implantation for 60 min at room temperature, 300,

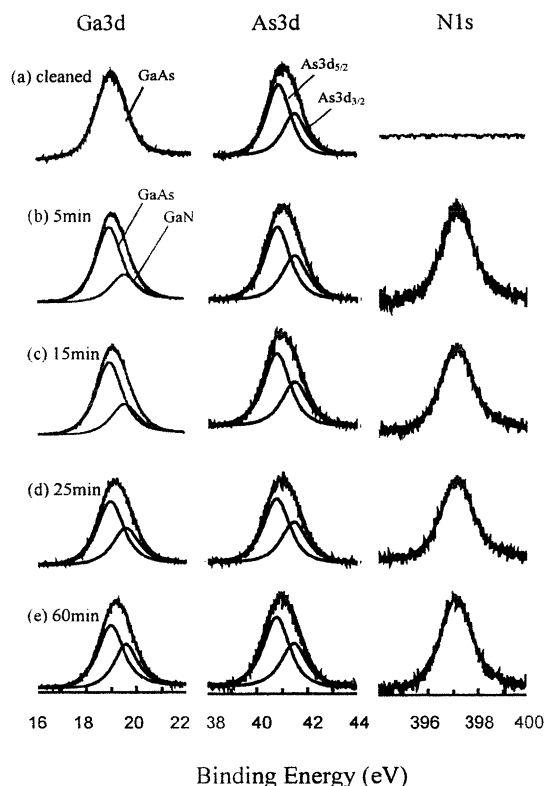


Fig. 2. (a) XPS spectra after 1 keV, 18 μ A Ar^+ bombardment of GaAs surface for 5 min Ga 3d, As 3d, and N 1s XPS spectra of GaAs nitrided at 300°C for, (b) 5 min; (c) 15 min; (d) 25 min; (e) 60 min, respectively.

450, and 600°C, respectively. A broadened Ga 3d peak and an obvious N 1s peak at the binding energy of 397.0 eV is observed in Fig. 3(b)–(e) due to Ga–N bond formation after N_2^+ implantation. Additionally, it can be seen that there is a temperature-dependence in the nitridation process. Plots of nitridation time and substrate temperature-dependence of the $[\text{N}]/[\text{Ga}]$ and $[\text{As}]/[\text{Ga}]$ atomic ratios are presented in Fig. 4(a) and 4(b), respectively. At room temperature, 300, and 450°C, nitridation proceeds quickly and reaches saturation at a $[\text{N}]/[\text{Ga}]$ atomic ratio of between from 0.58 to 0.65 after 25 min. At 600°C however, the initial nitridation takes place more quickly reaching a maximum $[\text{N}]/[\text{Ga}]$ ratio of 0.66 after 5 min nitridation. The $[\text{N}]/[\text{Ga}]$ ratio subsequently decreases to 0.52 after 25 min nitridation. The saturation $[\text{N}]/[\text{Ga}]$ atomic ratio indicates that nitridation is a self-limiting process. Corresponding to the change

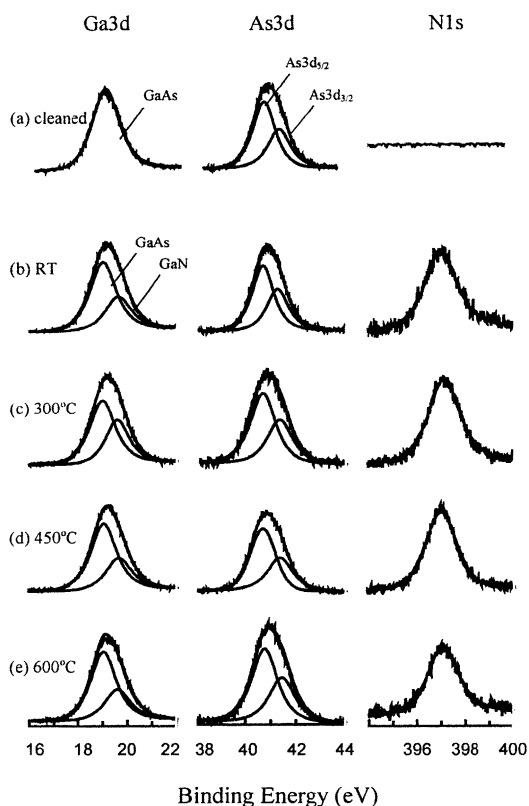


Fig. 3. (a) XPS spectra after 1 keV, 18 μA Ar^+ bombardment of GaAs surface for 5 min. XPS spectra of GaAs surface nitrided by 1.2 keV N_2^+ bombardment for 60 min at (b) room temperature; (c) 300°C; (d) 450°C; (e) 600°C.

of $[\text{N}]/[\text{Ga}]$ atomic ratio with temperature and nitridation time, the $[\text{As}]/[\text{Ga}]$ atomic ratio also changes by falling sharply during the initial nitridation, as shown in Fig. 4(b). The sum of the atomic ratios $[\text{N}]/[\text{Ga}] + [\text{As}]/[\text{Ga}]$ however remains fairly constant at 1. This indicates that the nitride layer formed during this nitridation process may be the ternary compound, $\text{GaAs}_x\text{N}_{1-x}$ (x increases with depth), as reported by experimental [20–22] and theoretical [23] studies. The XPS curve fitting results also suggest the absence of any As–N, As–As or Ga–Ga bonds in all samples obtained under these ion-induced nitridation conditions. It has been reported that free As atoms exist in the nitride layer synthesized by N_2 , $\text{N}_2\text{--H}_2$ and $\text{N}_2\text{--NH}_3$ plasma bombardment on GaAs(0 0 1) surface [24,25] and the N 1s peak displays a shoulder at higher binding energy that is attributed to N–H or

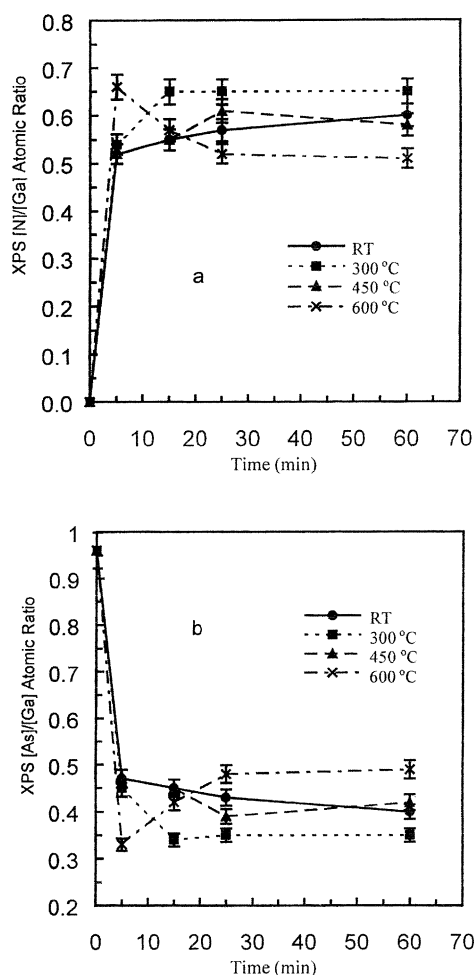


Fig. 4. Nitridation time and substrate temperature-dependence of: (a) the $[\text{N}]/[\text{Ga}]$ atomic ratio and (b) the $[\text{As}]/[\text{Ga}]$ atomic ratio.

N–N bonds. As–N bonds are detected in the nitride layer induced by atomic nitrogen implantation in GaAs(1 0 0) surface [26]. From an energetic point of view, group-III and group-V elements would tend to be nearest neighbors. The III–III (such as Ga–Ga) and V–V (such as As–As, As–N, N–N) bonds correspond to antisite defects, and have large formation energies. Theoretical calculations show that Ga–Ga and As–As bonds at {0 0 1} inversion domain boundaries cost, respectively, 0.37 ± 0.17 and 0.56 ± 0.17 eV more compared to normal Ga–As bonds [27], with the “uncertainty” reflecting the range of the chemical potentials. Calculating the N–N and As–As bond

formation energies by using the ab initio LMTO–ASA method with Löwdin perturbation technique ([28] and this work), we found that the average energy cost for Ga–Ga and N–N bonds is 2.86 eV per atom more than normal Ga–N bonds, and for Ga–Ga and As–N bonds is 0.32 eV per atom more than the GaAs + GaN(1 + 1) alloy. Therefore, such III–III and V–V bonding are unlikely to occur as indicated by our experimental results.

3.2. Depth profile analysis of the nitride films

Fig. 5 shows the [N]/[Ga] atomic ratio of the nitride films as a function of depth obtained by XPS depth profiling. Below 300°C, higher nitridation temperature leads to the larger thickness of nitride films and higher N concentration at the nitrided surfaces. However, when the nitridation temperature is above 300°C, both of nitride layer thickness and N concentration at nitrided surfaces decrease with temperature. This is different from other results obtained using N_2-NH_3 bombardment which show that the higher temperature, the thicker the nitride film on GaAs surface [20,24]. This suggests that the effect of GaAs surface temperature on the ion nitridation kinetics is significantly different from that in plasma nitridation.

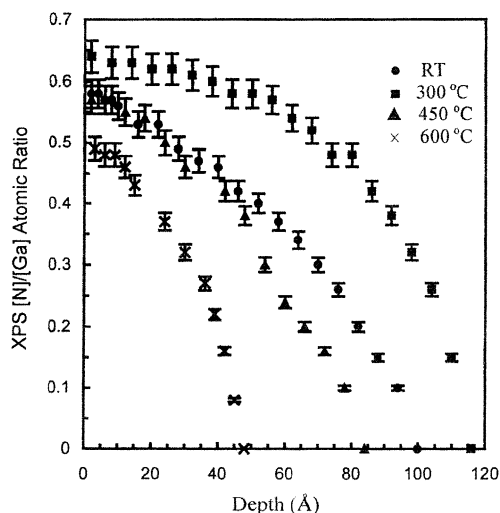


Fig. 5. Depth-dependence of the [N]/[Ga] atomic ratio for the nitrided layers formed by nitridation with 1.2 keV N_2^+ bombardment for 60 min at RT, 300, 450, and 600°C.

3.3. AFM images of the nitrided film surfaces

Fig. 6(b)–(f) show typical AFM images of nitrided GaAs surfaces under different N_2^+ bombardment conditions. The corresponding plots illustrating the effect of nitridation temperature and time on surface roughness (rms value) is shown in Fig. 7. The plots indicate that surface roughness strongly depends on substrate temperature. There is little increase in rms roughness values of samples nitrided at low temperature ($T < 450^\circ\text{C}$). A rms value of 0.48 nm is measured for the sample nitrided at 450°C for 25 min (Fig. 6(d)). For 60 min nitridation at 450°C, the rms roughness value increases to 1.1 nm. However, for nitridation at 600°C, rms roughness value increases significantly, reaching a value of 34.6 nm after 90 min. Similar trends have been reported for the plasma nitridation of GaAs [29]. Fig. 6(e) and Fig. 6(f) are the AFM images at 600°C for 5 and 25 min nitridation, respectively. The results show that the kinetics of high temperature ($T \approx 600^\circ\text{C}$) nitridation are different from that at low temperatures ($T < 450^\circ\text{C}$), and involves significant migration of surface atoms to form islands.

3.4. GaAs nitridation mechanism

The different chemical composition and surface morphology, as revealed by XPS and AFM measurements, of the nitrided layer formed under different nitridation parameters implies that nitridation temperature is of vital importance. In the plasma nitridation of GaAs, Losurdo and co-workers [24] simply envisaged the overall chemistry of the GaAs nitridation as $\text{GaAs} + \text{N} \rightarrow \text{GaN} + \text{As}$, and analyzed the framework of the heterogeneous reactions by considering the following steps: (i) chemisorption of nitriding species first on the GaAs surface and afterwards on the nitrided layer surface; (ii) inward migration of N atoms through the nitrided layer toward the $\text{GaAs}_{1-x}\text{N}_x/\text{GaAs}$ interface, followed by the exchange reaction of As with N at the $\text{GaAs}_{1-x}\text{N}_x/\text{GaAs}$ interface; (iii) desorption and outward migration of the As products, via Fickian diffusion. Unlike the plasma nitridation of GaAs, the detailed formation mechanism of Ga–N bonds during N_2^+ nitridation of GaAs at lower pressures may be different. The ion-assisted deposition under net sputtering conditions has been

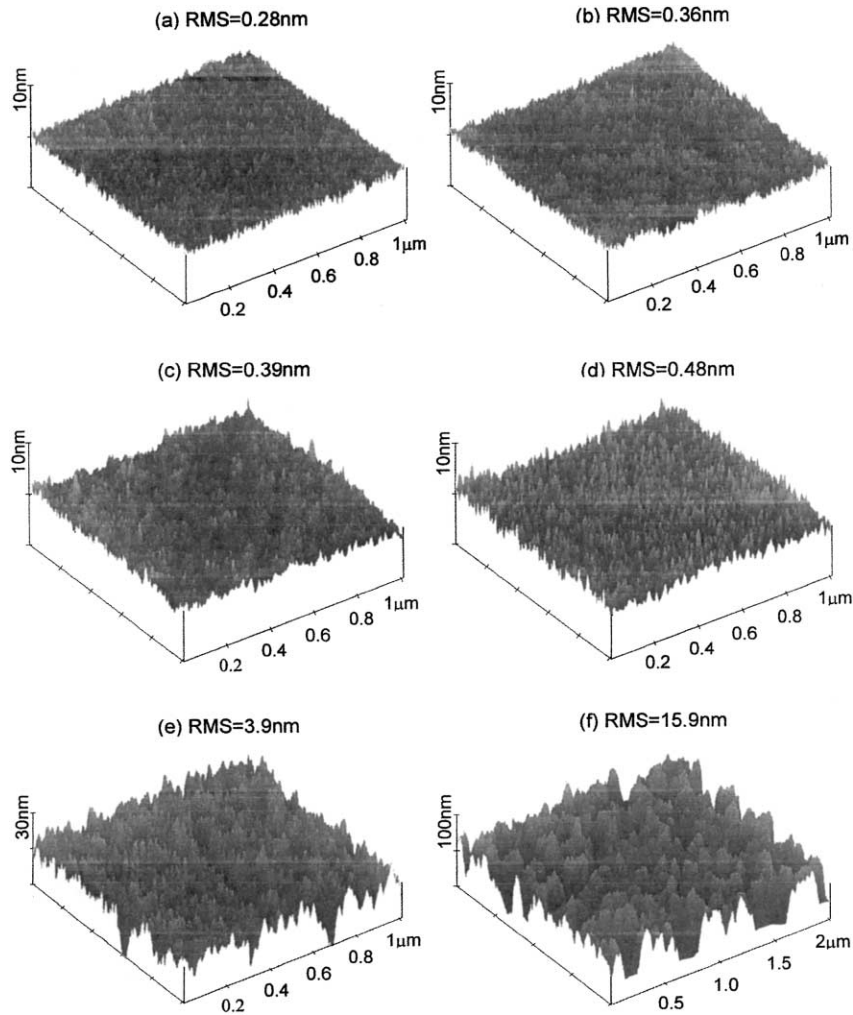


Fig. 6. AFM images with rms roughness of: (a) solution cleaned GaAs; GaAs nitrided by N_2^+ for (b) 5 min at 300°C; (c) 5 min at 450°C; (d) 25 min at 450°C; (e) 5 min at 600°C; (f) 25 min at 600°C.

described theoretically by an altered layer model proposed by Carter and co-workers [30], in which the bombarded substrate has three regions: (a) sputtered surface layer; (b) altered layer; (c) bulk. Based on the altered layer model, when the formation and sputtering of the nitride is in dynamic equilibrium, the N content and the nitrided layer thickness remain constant. The formation of the nitrided layer depends on N_2^+ implantation and sputtering in the altered layer, atom diffusion in the nitrided layer, and N atom incorporation at the $GaAs_{1-x}N_x/GaAs$ interface. The time-dependent and the steady-state concentration ratios of atomic species incorporated into a substrate

are modeled theoretically. However, this altered layer model treats the ion-assisted deposition as a physical process, and the chemical processes that are related directly to the formation of nitride layer are not included.

In order to interpret the formation and growth of nitride layers taking into account the chemical processes during ion-assisted nitridation, we propose the following mechanism for $GaAs_xN_{1-x}$ formation. First, as the Ar^+ -cleaned GaAs surface is Ga-rich, it is reactive to the deposited N species on the surface, N_2^+ is first trapped by Ga on the Ar^+ -cleaned GaAs surface, and Ga–N bonds is formed by the overall

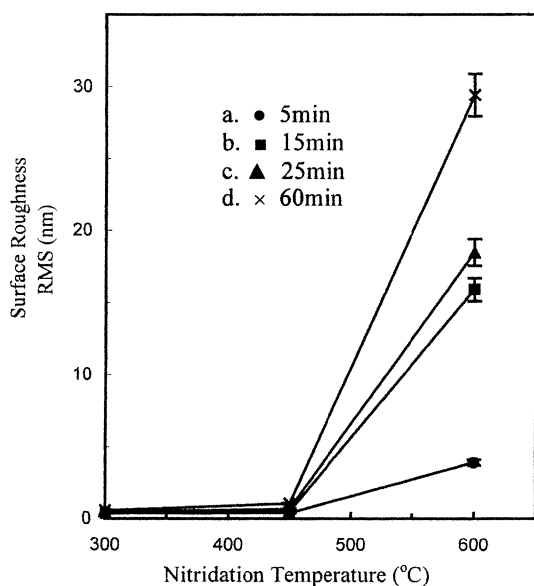


Fig. 7. Roughness (rms) for nitrided GaAs(1 0 0) surface as a function of nitridation temperatures (300, 450, 600°C) using nitridation times of: (a) 5 min; (b) 15 min; (c) 25 min; (d) 60 min.

reaction $2\text{Ga} + \text{N}_2^+ \rightarrow 2\text{GaN}$. However, when the N species begin to replace As dimers on the surface layer, the following reaction occurs: $2\text{GaAs} + \text{N}_2^+ \rightarrow 2\text{GaN} + 2\text{As}$. The most of the substituted As will desorb under N_2^+ bombardment, however, some of them will take the positions left by the segregation of As in the nitride layer. N species accumulated on the surface penetrate to the subsurface and deeper layers. Since the formation energy of GaN is lower than that of GaAs [14], the nitridation proceeds with the N species forming bonds with Ga atoms and replacing As atoms in the second (or deeper) layers via the reaction: $\text{GaAs} + \text{N} \rightarrow \text{GaN} + \text{As}$.

Sputtering of the nitrided films occurs while at the same time N atoms diffuse to the $\text{GaAs}_{1-x}\text{N}_x/\text{GaAs}$ interface through the nitrided layer terminating with the N–As exchange reaction at the $\text{GaAs}_{1-x}\text{N}/\text{GaAs}$ interface. The free As produced during this exchange reaction diffuses to the surface and are sputtered away. Finally, a dynamic equilibrium between formation and sputtering of the nitrided layer is attained, and the N concentration and the nitrided layer thickness reach saturation.

Since the diffusivity increases with temperature, we expect the N diffusion length, and hence nitride layer

thickness, to increase at higher temperatures. However, calculations for N-to-As exchange in GaAs indicates that the substitution energy becomes higher deeper in the film [21]. The nitride layer thickness and N distribution as shown in Fig. 5 depend on temperature, indicating that nitridation of GaAs is a self-limiting process. Fig. 5 also shows that at low temperatures, N diffusion is more significant than sputtering, vaporization, and decomposition. Hence, both the thickness of the nitride layer and N concentration in the nitride layers increase with temperature. The thickest nitrided layers with highest $[\text{N}]/[\text{Ga}]$ atomic ratio are obtained at 300°C. When $T \geq 450^\circ\text{C}$, vaporization and decomposition of the surface [31,32] result in reduced incorporation of N atoms.

The thermal decomposition of GaAs when it is heated higher than 550°C has been reported in [31,33]. The morphological changes to the AFM images of the nitrided layers at 600°C (Fig. 6(e) and (f)) are believed to be relative to GaAs thermal decomposition and increased mobility of surface atoms. GaAs thermal decomposition leads more active Ga sites. At high temperatures, diffusion of surface Ga and N atoms result in nucleation of $\text{GaAs}_{1-x}\text{N}_x$ islands whose sizes increase rapidly with time.

4. Conclusions

In situ XPS analysis shows that Ar^+ cleaning of the GaAs(1 0 0) surface results in a Ga-rich GaAs (1 0 0) surface which is amenable to ion nitridation using 1.2 keV N_2^+ . Free Ga, As, and As–N are not detected by XPS in the nitrided layers. The ion-induced nitridation of GaAs(1 0 0) is a self-limiting process. At low temperatures ($<450^\circ\text{C}$), the degree of nitridation increases with temperature and a relatively smooth $\text{GaAs}_{1-x}\text{N}_x$ film is obtained. High temperature nitridation ($>450^\circ\text{C}$) results in a reduction in the degree of nitridation of the GaAs and the nucleation of $\text{GaAs}_{1-x}\text{N}_x$ islands.

Acknowledgements

The author thanks J.S. Pan and J.W. Chai of the Institute of Materials Research and Engineering (IMRE) for their help with the XPS depth profile

measurements. Helpful discussions with E.S. Tok are also gratefully acknowledged.

References

- [1] H. Morkoc, S. Strite, G.B. Gao, M.E. Lin, B. Sverdlov, M. Burns, *J. Appl. Phys.* 76 (1994) 1363.
- [2] H.P. Maruska, J.J. Tietjen, *Appl. Phys. Lett.* 15 (1969) 327.
- [3] E. Kim, I. Berishev, A.V. Bensaoula, S. Lee, S.S. Perry, K. Waters, J.A. Schultz, *Appl. Phys. Lett.* 71 (1997) 3072.
- [4] T. Lei, M. Fanciulli, R.J. Molnar, T.D. Moustakas, R.J. Graham, J. Scanlon, *Appl. Phys. Lett.* 59 (1991) 944.
- [5] V. Dmitriev, K. Irvine, G. Bulman, J. Edmond, A. Zubrilov, V. Nikolaev, I. Nikitina, D. Tsvetkova, A. Babsnin, A. Sitnikova, Y. Muskin, N. Bert, *J. Cryst. Growth* 166 (1996) 601.
- [6] O. Brandt, H. Yang, K.H. Ploog, *Phys. Rev. B* 54 (1996) 4432.
- [7] M.E. Lin, S. Strite, A. Agarwal, A. Salvador, G.L. Zhou, N. Teraguchi, A. Rockett, H. Morkoc, *Appl. Phys. Lett.* 62 (1993) 702.
- [8] M. Mizuta, S. Fujieda, Y. Matsumoto, T. Kawamura, *Jpn. Appl. Phys.* 25 (1986) L945.
- [9] S. Strite, J. Ruan, Z. Li, N. Manning, A. Salvador, H. Chen, D.J. Smith, W.J. Choyke, H. Morkoc, *J. Vac. Sci. Technol. B* 9 (1991) 1924.
- [10] A. Strittmatter, A. Krost, M. Straßburg, V. Turck, D. Bimberg, *Appl. Phys. Lett.* 74 (1999) 1242.
- [11] T. Lei, T.D. Moustakas, R.J. Graham, Y. He, S.J. Berkowitz, *J. Appl. Phys.* 71 (1992) 4933.
- [12] L.A. Delouise, *J. Vac. Sci. Technol. A* 11 (1993) 609.
- [13] N. Herbot, O.C. Hellman, P. Ye, X.D. Wang, O. Vancauwenberghe, in: J.W. Rabalais (Ed.), *Lower Energy Ion-Surface Interactions*, Wiley, New York, 1994, p. 387.
- [14] O. Vancauwenberghe, O.C. Hellman, N. Herbots, J.L. Olson, W.J. Croft, in: J.M.E. Harper, K. Miyake, J.R. McNeil, S.M. Gorbalkin (Ed.), *Lower Energy Ion Beam Plasma Modification Materials*, Pittsburgh, PA, 1991, Mater. Res. Soc. Symp. Proc. 233.
- [15] O. Kubaschewski, C.B. Alcock, *Metallurgical Thermochemistry*, 5th Edition, Pergamon Press, New York, 1979.
- [16] J.S. Pan, C.H.A. Huan, A.T.S. Wee, H.S. Tan, K.L. Tan, *J. Mater. Res.* 13 (1998) 1799.
- [17] I.L. Singer, J.S. Murday, L.R. Cooper, *Surf. Sci.* 108 (1984) 7.
- [18] J.F. Moulder, W.F. Stickle, P.E. Sobol, K.D. Bomben, in: J. Chastain (Ed.), *Handbook of X-ray Photoelectron Spectroscopy*, Perkin-Elmer Corporation, Eden Prairie, MN, 1992.
- [19] L.A. Delouise, *J. Vac. Sci. Technol. A* 10 (1993) 1637.
- [20] M.E. Jones, J.R. Shealy, J.R. Engstrom, *Appl. Phys. Lett.* 67 (1995) 542.
- [21] S.B. Zhang, A. Zunger, *Appl. Phys. Lett.* 71 (1997) 677.
- [22] M. Wayers, M. Sato, H. Ando, *J. Appl. Phys.* 31 (2) (1992) L853.
- [23] A. Masuda, Y. Yonezawa, A. Morimoto, T. Shimizu, *Jpn. J. Appl. Phys.* 34 (1) (1995) 1075.
- [24] M. Losurdo, P. Capezzuto, G. Bruno, E.A. Irene, *Phys. Rev. B* 58 (1998) 15878.
- [25] Y.J. Park, E.K. Kim II, K. Han, S.-K. Min, P. O’Keeffe, H. Mutoh, H. Munkata, H. Kukimoto, *Appl. Surf. Sci.* 117/118 (1997) 551.
- [26] P. Hill, J. Lu, L. Haworth, D.I. Westwood, J.E. Macdonald, *Appl. Surf. Sci.* 123/124 (1998) 126.
- [27] W.R.L. Lambrecht, C. Amador, B. Segall, *Phys. Rev. Lett.* 68 (1992) 1363.
- [28] J.-C. Zheng, C.H.A. Huan, A.T.S. Wee, R.-Z. Wang, Y.-M. Zheng, *J. Phys.: Condens. Matter* 11 (1999) 927.
- [29] P. Hill, D.I. Westwood, L. Haworth, J. Lu, J.E. Macdonald, *J. Vac. Sci. Technol. B* 15 (1997) 1133.
- [30] G. Carter, I.V. Katardjiev, M.J. Nobes, *Vacuum* 38 (1988) 117.
- [31] M. Losurdo, P. Capezzuto, G. Bruno, P.R. Lefebvre, E.A. Irene, *J. Vac. Sci. Technol. B* 16 (1998) 2665.
- [32] R.J. Hauentein, D.A. Collins, X.P. Cai, M.L. O’Steen, T.C. McGill, *Appl. Phys. Lett.* 66 (1991) 2861.
- [33] S. Gourrier, L. Sinit, P. Friedel, P.K. Larsen, *J. Appl. Phys.* 54 (1983) 3993.